

# Anti-Inflammatory Effects and Molecular Mechanisms of Shenmai Injection in Treating Acute Pancreatitis: Network Pharmacology Analysis and Experimental Verification

Yanqiu He<sup>1,\*</sup>, Cheng Hu<sup>1,\*</sup>, Shiyu Liu<sup>1</sup>, Mingjie Xu<sup>1</sup>, Ge Liang<sup>2</sup>, Dan Du<sup>3</sup>, Tingting Liu<sup>1</sup>, Fei Cai<sup>1</sup>, Zhiyao Chen<sup>1</sup>, Qingyuan Tan<sup>1</sup>, Lihui Deng<sup>1</sup>, Qing Xia<sup>1</sup>

<sup>1</sup>Pancreatitis Centre, Department and Laboratory of Integrated Traditional Chinese and Western Medicine, West China Hospital, Sichuan University, Chengdu, People's Republic of China; <sup>2</sup>Laboratory of Clinical Proteomics and Metabolomics, Institutes for Systems Genetics, Frontiers Science Center for Disease-Related Molecular Network, West China Hospital, Sichuan University, Chengdu, People's Republic of China; <sup>3</sup>Advanced Mass Spectrometry Center, Research Core Facility, Frontiers Science Center for Disease-Related Molecular Network, West China Hospital, Sichuan University, Chengdu, People's Republic of China

\*These authors contributed equally to this work

Correspondence: Lihui Deng, Pancreatitis Centre, Department and Laboratory of Integrated Traditional Chinese and Western Medicine, West China Hospital, Sichuan University, Chengdu, People's Republic of China, Email [denglihui@scu.edu.cn](mailto:denglihui@scu.edu.cn)

**Background:** Acute pancreatitis (AP) is an inflammatory disorder of the exocrine pancreas without specific treatment. Shenmai injection (SMI) was reported to eliminate the severity of experimental AP. This study aimed to explore the mechanisms underlying the synergistic protective effects of SMI on AP based on network pharmacology and experimental validation.

**Methods:** Network pharmacology analysis and molecular docking based on identified components were performed to construct the potential therapeutic targets and pathways. The principal components of SMI were detected via ultra-high-performance liquid chromatography-coupled with quadrupole time-of-flight mass spectrometry (UHPLC-QTOF/MS). Effect of SMI and the identified components on cellular injury and IL6/STAT3 signaling was assessed on mouse pancreatic acinar cell line 266–6 cells. Finally, 4% sodium taurocholate (NaT) was used to induce AP model to assess the effects of SMI in treating AP and validate the potential molecular mechanisms.

**Results:** By searching the TCMSP and ETCM databases, 119 candidate components of SMI were obtained. UHPLC-QTOF/MS analysis successfully determined the representative components of SMI: ginsenoside Rb1, ginsenoside Rg1, ginsenoside Re, and ophiopogonin D. Fifteen hub targets and eight related pathways were obtained to establish the main pharmacology network. Subnetwork analysis and molecular docking indicated that the effects of these four main SMI components were mostly related to the interleukin (IL) 6/STAT3 pathway. In vitro, SMI, ginsenoside Rb1, ginsenoside Rg1, ginsenoside Re, and ophiopogonin D increased the cell viability of NaT-stimulated mouse pancreatic acinar 266–6 cells and decreased IL6 and STAT3 expression. In vivo, 10 mL/kg SMI significantly alleviated the pancreatic histopathological changes and the expression of IL6 and STAT3 in the AP mice.

**Conclusion:** This study demonstrated SMI may exert anti-inflammatory effects against AP by suppressing IL6/STAT3 activation, thus providing a basis for its potential use in clinical practice and further study in treating AP.

**Keywords:** acute pancreatitis, Shenmai injection, network pharmacology, molecular docking, IL6/STAT3 signaling pathway

## Introduction

Acute pancreatitis (AP) is one of the most common gastrointestinal diseases, with an estimated cost of approximately 2.6 billion dollars annually and the global incidence is still increasing.<sup>1,2</sup>

Intra-acinar events leading to the inflammatory cascade amplify systemic inflammatory response syndrome and ultimately lead to multiple organ dysfunction syndromes and death. Severe AP is characterized by persistent organ

failure with a substantial mortality rate of 36–50% and causing the reduced quality of life and significant socio-economical burden.<sup>3–5</sup> Recent network meta-analysis that included 7366 participants in 78 randomized controlled trials assessing the effects of pharmacological interventions on AP found no consistent clinical benefits from any interventions.<sup>6</sup> Current guidelines recommended routine methods for managing AP.<sup>7,8</sup>

Traditional Chinese medicine (TCM) has been clinically applied for thousands of years in China and has been demonstrated to be effective and safe for treating AP in clinical practice.<sup>9</sup> The underlying mechanism of TCM in treating AP remains unclear. Based on TCM theory, AP is triggered by invasion of “heat-evil” to the organs. We proposed the therapeutic principles that require “nourishing Qi and Yin, removing blood stasis, clearing heat, removing toxins and purgation” (abbreviated as the “Yi-Huo-Qing-Xia” methods) for AP.<sup>10–12</sup> Studies have investigated treatments that involve “clearing heat, removing toxins and purgation”, which include prescriptions for dachengqi decoction, chiqinchenqi decoction, and qingyi decoction.<sup>13–20</sup> Notably, the progression of heat-toxins and associated treatments tend to injure the Qi and Yin, resulting in qi-yin deficiency. Therefore, nourishing Qi and Yin is important for treating AP. Nevertheless, few studies have focused on nourishing Qi and Yin in the early stages of AP.

Shenmai injection (SMI), a formula derived from the prescription Shendong yin,<sup>21</sup> is a sterile product extracted and purified from Chinese medicinal materials under the guidance of TCM theory and modern pharmaceutical manufacturing technologies. It is one of the main formulas for nourishing Qi and Yin.<sup>22,23</sup> SMI is indicated as an adjuvant treatment for shock, coronary disease, and chronic pulmonary cardiac disease and is recommended by the National Health Commission of China for severe or critical coronavirus disease (COVID-19) (2020).<sup>24</sup> A previous study showed that SMI reduced the severity of experimental AP.<sup>25</sup> Nevertheless, the individual components responsible for the various pharmacological responses and potential mechanisms of SMI on AP remain unclear.

Here, we investigated the possible anti-inflammatory role and mechanisms of SMI in treating AP by integrating network pharmacology, molecular docking analysis and experimental validation. [Figure 1](#) presents a flowchart of the study design.

## Materials and Methods

### SMI Drug Component Screening

All components of *Panax ginseng* and *Radix Ophiopogonis* were determined from the Traditional Chinese Medicine Systems Pharmacology Database and Analysis Platform (TCMSP; <https://tcmispw.com/>) and the Encyclopedia of Traditional Chinese Medicine (ETCM; <http://www.tcmip.cn/ETCM/index.php/Home/Index>).

### Major SMI Components Identified via Ultra-High-Performance Liquid Chromatography-Coupled with Quadrupole Time-of-Flight Mass Spectrometry (UHPLC-QTOF/MS) Analysis

Based on the previously screened active components and the reported main pharmacologically active components,<sup>26,27</sup> we performed UHPLC-QTOF/MS analysis to verify the predominant identified components of SMI were available in the sample used for subsequent experiments.

### SMI and Standards

SMI is a Chinese patent drug extracted from *Panax ginseng* (*Panax ginseng* C.A. Mey, steamed and dry) and *Ophiopogon japonicus* (*Ophiopogon japonicus* [L.f.] Ker-Gawl, root). SMI was produced by Sichuan Chuanda West China Pharmaceutical Co., Ltd. (Chengdu, China) and purchased from outpatient pharmacy of West China Hospital. *Panax ginseng* and *Ophiopogon* root standards were purchased from Chengdu Push Bio-Technology Co., Ltd. (Chengdu, China) and maintained at 25°C. [Table 1](#) provides the detailed information on the material medica from SMI. [Supplementary Table 1](#) provides the detailed information on the reagents and natural compound standards.

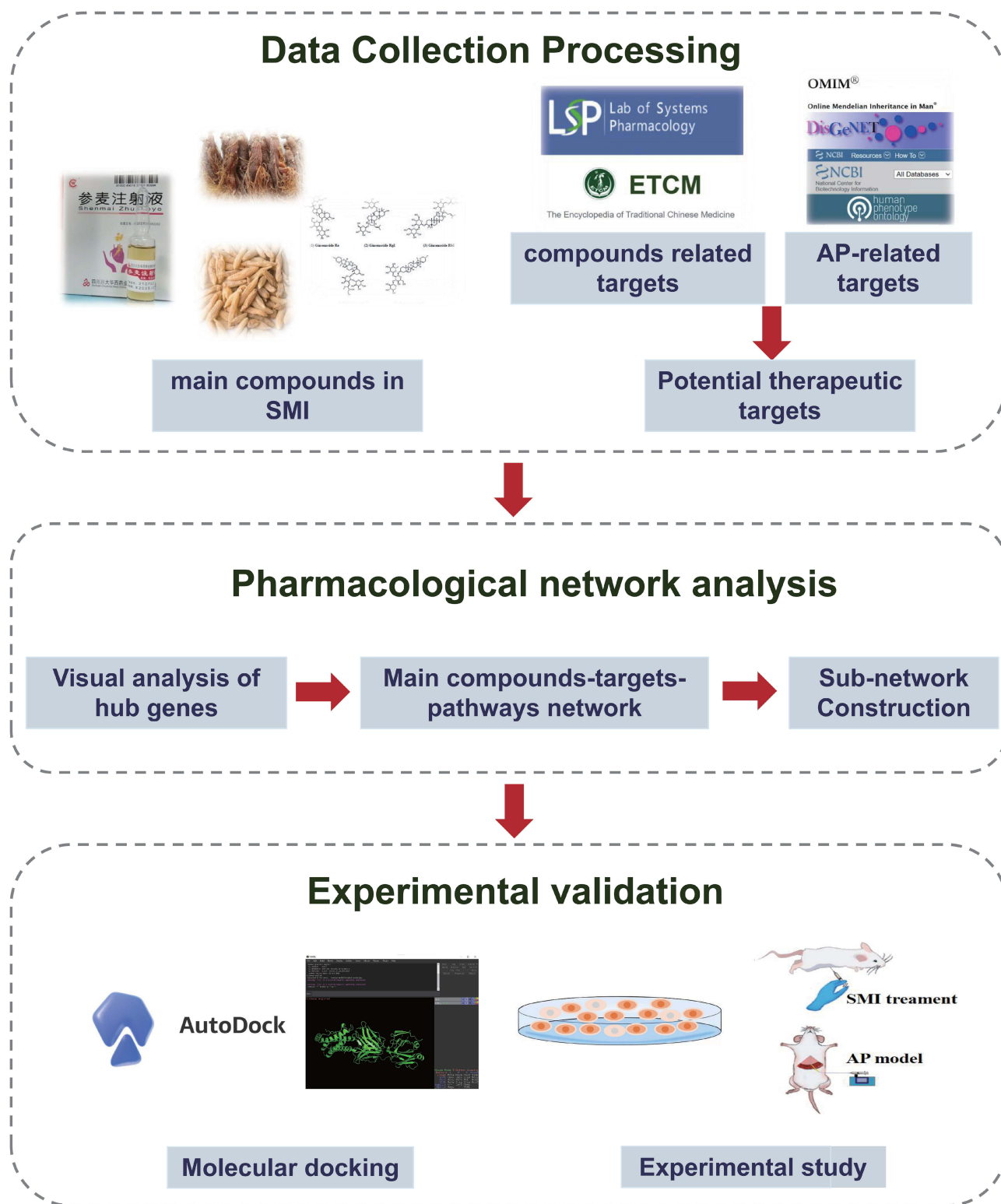


Figure 1 Study flowchart.

## UHPLC-QTOF/MS Analysis of SMI and Standard

SMI was centrifuged at 13,000 r/min for 3 min, and 10  $\mu$ L of the supernatant was taken for testing. Standards were dissolved in methanol and obtained as a 1  $\mu$ g/mL solution. The SMI and standards were analyzed on a UHPLC (Nexera

**Table 1** Basic Information of Two Medicinal Materials of SMI

Chinese Name	English Name	Latin Name	Family
Hongshen	Red Ginseng	<i>Panax ginseng</i> C.A. Mey	Araliaceae
Maidong	<i>Ophiopogon japonicus</i>	<i>Ophiopogon japonicus</i> (L.f) Ker-Gawl	Liliaceae

LC-30A, Shimadzu Corporation, Kyoto, Japan) with a Q-TOF MASS instrument (X500R, AB SCIEX™). Separation was performed on a BEH C18 column (100×2.1 mm, 3 μm, Waters) at 40°C with a flow rate of 0.5 mL/min. The mobile phase consisted of water containing 0.1% formic acid and acetonitrile and was performed with the following gradient elution program: 0 min, 90% A, 10% B; 6 min, 5% A, 95% B; 8 min, 5% A, 95% B; 8.1 min, 90% A, 10% B; 10 min, 90% A, 10% B. The injection volume was 10 μL.

The Q-TOF-MS system was operated using an electrospray ionization source in negative mode with the following operating parameters: ion source gas1 (gas 1): 50, ion source gas2 (gas 2): 50, curtain gas: 35, source temperature: 500° C, ion spray voltage floating: 4500 V, TOF MS scan range: 200–1200 Da, product ion scan range: 50–1200 Da, TOF MS scan accumulation time 0.2 s, and product ion scan accumulation time: 0.01 s. The secondary mass spectrum was acquired by information-dependent acquisition, in high-sensitivity mode, with declustering potential: ±60 V and collision energy: 35±15e V. All data were processed using SCIEX OS-MQ 2.1 (AB SCIEX™).

## Drug Compound-Related Target Screening

The canonical SMILES structure formats of the compounds were obtained from the PubChem database (<https://pubchem.ncbi.nlm.nih.gov/>), and the compound targets were identified by inputting them into the Swiss Target Prediction database (<http://www.swisstargetprediction.ch/>) with the species limited to “Homo sapiens” and “probability >0”.

## AP-Related Target Screening

AP-associated targets were identified using “acute pancreatitis” as the keyword in the OMIM (<https://www.omim.org/>), DisGeNet (<http://www.disgenet.org>), HPO (<https://hpo.jax.org/app/>), and NCBI (<https://www.ncbi.nlm.nih.gov/>) databases. Protein names of all targets were converted into official gene symbols using UniProt (<https://www.uniprot.org/>). After removing duplicated genes, the potential therapeutic targets of SMI were collected and further visualized in the Evvnn database (<http://www.ehbio.com/test/venn/#/>).

## Protein–Protein Interaction (PPI) Network Analysis

The PPI network of the potential therapeutic targets was constructed and analyzed using the STRING database (<https://string-db.org/>) with the species limited to “Homo sapiens” and a confidence score >0.7. The results were saved as TSV files and further visualized in Cytoscape 3.7.2. In the PPI network, targets with high degrees played vital roles in the central correlation. We considered the targets with degree values greater than the median as the main targets.

## Gene Ontology (GO) and Kyoto Encyclopedia of Genes and Genomes (KEGG) Pathway Enrichment Analysis

The DAVID 6.8 database (<https://david.ncifcrf.gov/>) was used to perform GO annotation and KEGG pathway enrichment analysis of the potential therapeutic targets. The results were visualized using the bioinformatics platform (<http://www.ehbio.com/ImageGP/>).

## Pharmacology Network Construction and Analysis

From the previously obtained main targets and enriched pathways, we constructed the compounds-targets-pathways network as the main pharmacology network. The interleukin (IL) 6/STAT3 pathway was selected from the PPI network analysis and KEGG signaling pathways. A subnetwork of IL6/STAT3 pathways-targets-compounds was extracted from the main network.

## Molecular Docking

Molecular docking was performed to visually investigate the interactions between the major identified components and the selected potential targets using AutoDock Vina 1.1.2. First, two-dimensional structures of the components were obtained from the PubChem database (<https://pubchem.ncbi.nlm.nih.gov>), then converted to three-dimensional structures in mol2 format by ChemOffice software to prepare the micromolecule ligand compounds. The components and main target proteins for docking were prepared using PyMOL 1.7.2.1 software and saved as PDBQT files. AutoDock Vina (<http://vina.scripps.edu/>) was used to perform molecular docking and calculate the binding affinity. The docking results for the active components and main protein targets were visualized with PyMOL software.

## Experimental Assessments

### Reagents

Sodium taurocholate (NaT) was from Sigma-Aldrich (#86339-5G, St. Louis, MO, USA). The following antibodies were used for Western blotting: phospho-STAT3 (Tyr705, #9145S), STAT3 (#12640S), anti-IL6 (#12912S) were purchased from Cell Signaling Technology (Danvers, MA, USA); anti- $\beta$ -actin (#66009-1-Ig) was from Proteintech (Wuhan, Hubei, China). Complete protease inhibitor cocktail (#05892791001) and phosphatase inhibitor cocktail (#04906845001) were from Roche (Mannheim, Germany). Bicinchoninic acid protein assay kit (#23225) was from Thermo Fisher (Rockford, Illinois, USA). Polyvinylidene difluoride membranes (#IPVH00010) and Ultra ECL Western Blotting Detection Reagent (#4AW011) were from 4A Biotech (Beijing 4A Biotech Co., Ltd). TRIzol Reagent (#15596026) was from life technologies (Waltham, MA, USA). The chemical standards for SMI contained components were purchased from Sichuan Push Bio-technology Co., Ltd. (Chengdu, Sichuan, China).

### Cellular Viability Assessment

To determine whether SMI has a protective effect on cells, we performed cellular viability tests. Cell counting kit-8 (CCK-8) was used to indicate the number of viable cells in the proliferation and cytotoxicity assays. Mouse pancreatic acinar cell line 266-6 (CRL-2151, ATCC, Manassas, VA, USA) was cultured in Dulbecco's modified Eagle's medium supplemented with 10% fetal bovine serum and 1% penicillin-streptomycin at 37°C with 5% CO<sub>2</sub>. The cells were seeded into 96-well plates at the same density, pretreated with SMI (1, 5, 10, or 20  $\mu$ L/mL) for 24 h, then incubated in medium containing NaT (5 mM) for 3 h. The CCK-8 assay was performed as per the manufacturer's instructions.

### Western Blots for IL6 and STAT3

Cells and pancreatic tissues were homogenized in RIPA buffer containing 50 mmol/L Tris (pH 7.4), 150 mmol/L NaCl, 1% sodium deoxycholate, 1% Triton X-100, 0.1% SDS, sodium orthovanadate, sodium fluoride, EDTA, leupeptin and a mix of protease and phosphatase inhibitors. Protein extracts were resolved by SDS-PAGE gel electrophoresis and transferred to polyvinylidene difluoride membranes. Then the membranes were blocked with 5% non-fat milk or 5% BSA for 1 h at room temperature, followed by incubation with primary antibodies overnight at 4°C and incubation with secondary antibodies for 1 hour at room temperature. Immuno-reactive bands were visualized by Chemiluminescent

**Table 2** Chromatography and Mass Spectrum for Components and the Corresponding Authentic Standards

Compound	Formula	RT (min)		Precursor (m/z)		Ion	Error (ppm)	MS/MS
		Standard	SMI	Standard	SMI			
Re	C48H82O18	2.959	2.980	991.552	991.553	[M+FA-H]-	0.706	945.543 799.485 637.433
RgI	C42H72O14	2.985	3.010	845.499	845.497	[M+FA-H]-	-3.075	845.487 799.483 637.431
RbI	C54H92O23	3.552	3.594	1153.622	1153.612	[M+FA-H]-	-8.668	1153.599 1107.593 600.300
D	C44H70O16	5.680	5.687	899.467	899.467	[M+FA-H]-	0	853.459 721.415 575.358
D'	C44H70O16	5.811	NA	899.467	899.467	[M+FA-H]-	NA	853.457 721.417

**Abbreviations:** RT, retention time; SMI, Shenmai injection; MS, mass spectrometry; Re, Ginsenoside Re; RgI, Ginsenoside RgI; RbI, Ginsenoside RbI; D, Ophiopogonin D; D', Ophiopogonin D'; NA, not applicable.

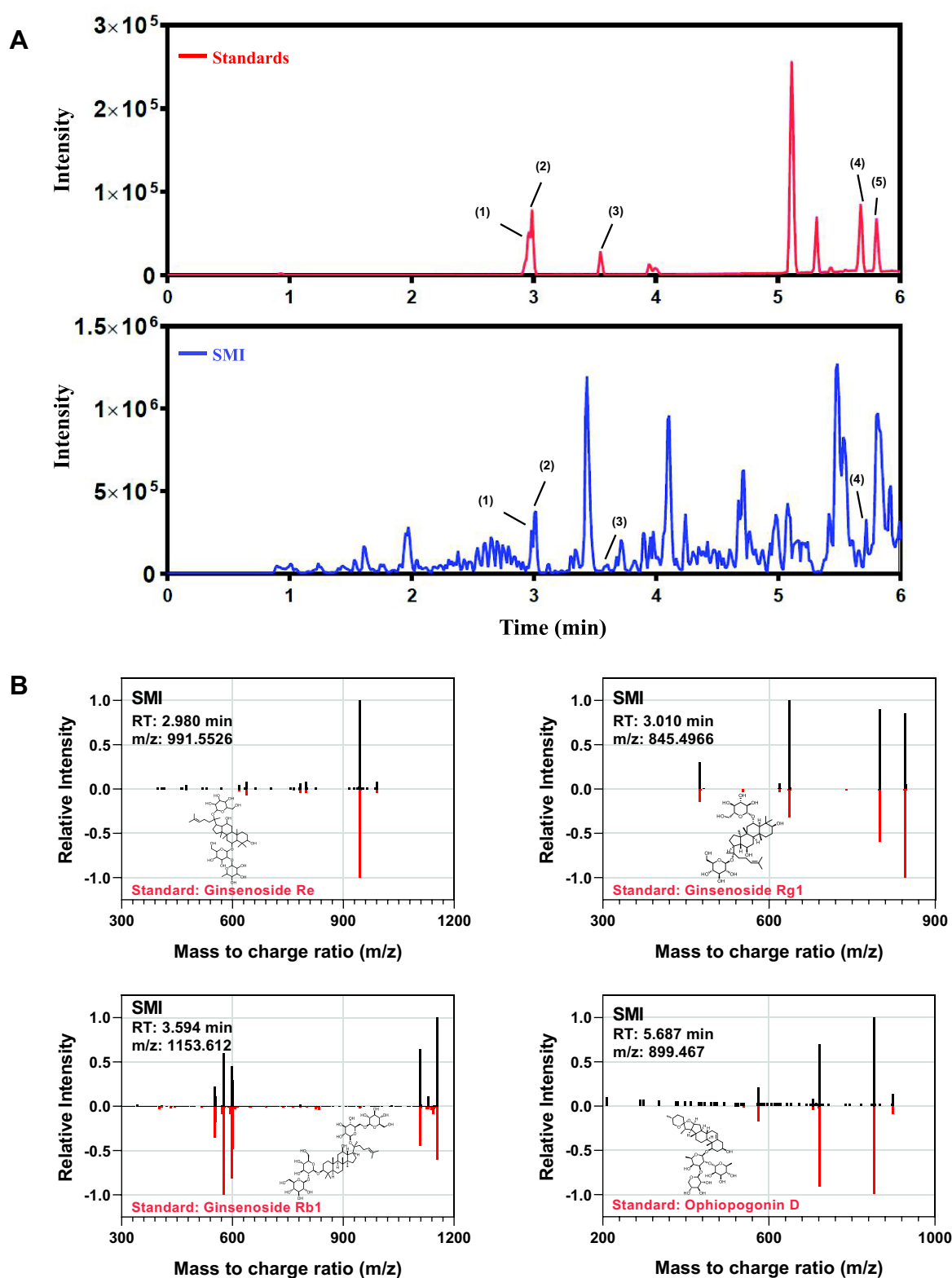


**Figure 2** Confirmation of the components of SMI by standard compounds. **(A)** Representative base peak intensity chromatograms of standards (red line) and SMI (blue line). **(B)** Measured MS/MS spectral fragmentation profiles of SMI (top, in black) matching chemical standards (bottom, in red).

Detection System (Bio-Rad; Hercules, CA, USA). To estimate protein levels, optical density values in each blot were expressed relative to those of the loading control ( $\beta$ -actin).

### Animals

Male C57BL/6J mice (weighing 22–25g) were purchased from Gempharmatech Co., Ltd. (Nanjing, China), maintained at  $22 \pm 2^\circ\text{C}$  on a 12-h light–dark cycle, and fed standard laboratory chow and water throughout the experiment. All animal experiments were performed in accordance with the guidelines approved by the Animal Ethics Committee of West China Hospital, Sichuan University (2021333A).

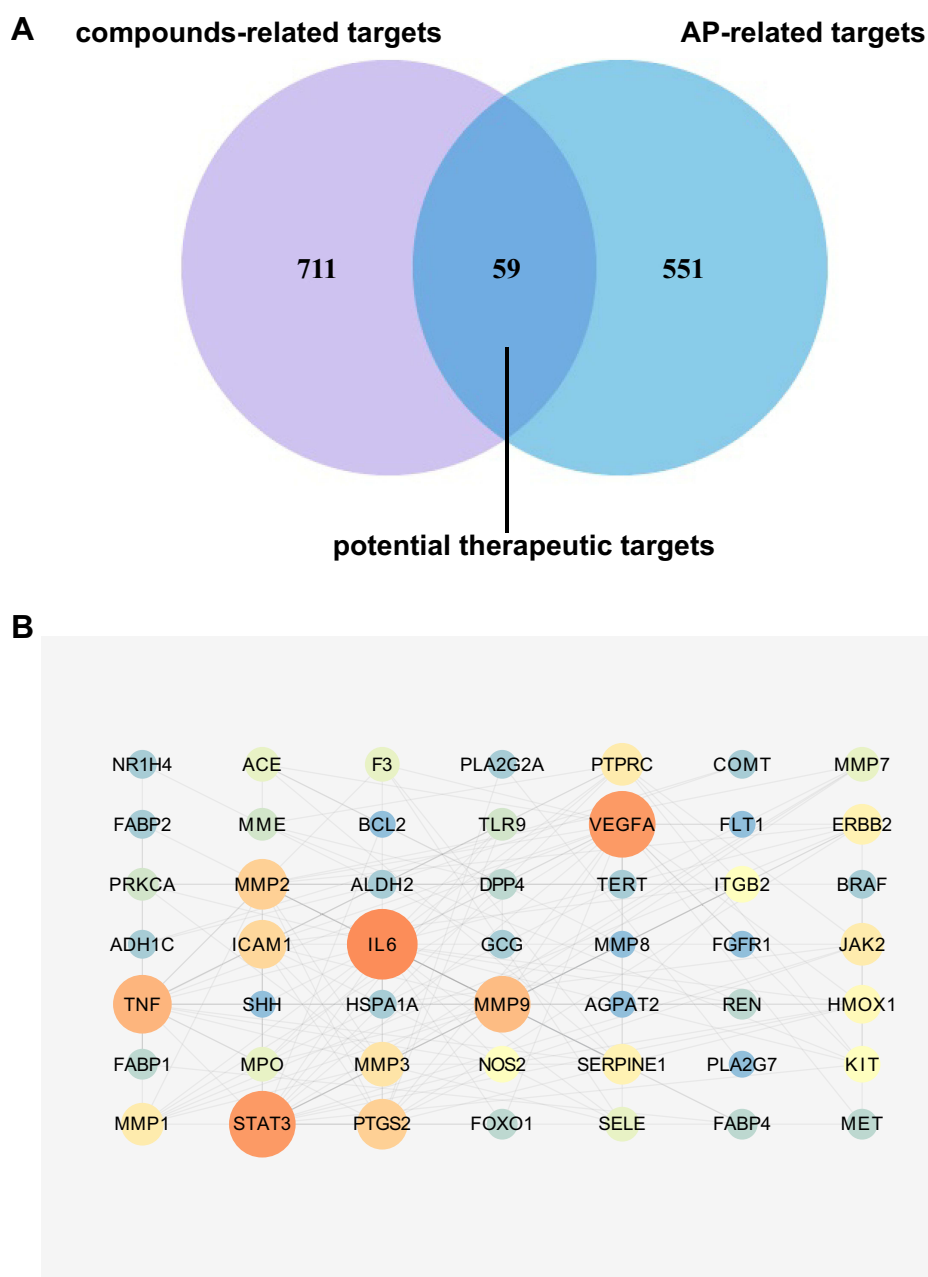


**Figure 3** Crosstalk between SMI and AP targets. **(A)** Venn diagram of compound-related target interactions overlapping with AP-related targets. **(B)** Protein–protein interaction network in the STRING database.

**Abbreviations:** SMI, Shenmai injection; AP, acute pancreatitis.

## AP Models and SMI Treatment

Mice were divided into control, AP and AP+SMI group, respectively (n = 8 in each group). AP-model mice were induced via retrograde pancreatic ductal injection with 4% sodium taurocholate (NaT) dissolved in saline. Briefly, mice were anesthetized with 2% isoflurane (gas flow: 0.5 L/min) using a vaporizer and gas scavenger system. Using sterile techniques, a small midline laparotomy incision was made. The duodenum was flipped to reveal its distal side and held in place by ligatures. The bile duct was identified, and a 30-gauge needle was inserted through the antimesenteric aspect of the duodenum to cannulate the biliopancreatic duct. NaT was infused at 5  $\mu$ L/min for 10 min using a perfusion pump (Pump33DDS, Harvard Apparatus, Holliston, MA, USA). Saline-infused mice served as controls. In the AP+SMI group, SMI (10 mL/kg) was injected intraperitoneally twice: pretreated within 24 h before NaT induction and 1 h after the procedure. Animals were euthanized 24 h after NaT induction, and relevant organs were harvested to assess the severity. Detailed protocols for the histopathological assessment of the pancreas were as previously described.

## Statistical Analysis

Data were analyzed using one-way analysis of variance and Tukey's post-hoc test for multiple comparisons with GraphPad Prism 8.0 software (GraphPad Software Inc., La Jolla, CA, USA). Data are presented as the mean  $\pm$  standard error of the mean. A two-sided  $p < 0.05$  was considered statistically significant.

## Results

### Acquiring the Components and Potential Targets

By searching the TCMS and ETCM databases, 119 candidate components of SMI were obtained ([Supplementary Table 2](#)). We then used UHPLC-QTOF/MS to determine the five reported active components of SMI with chemical standards by matching the accurate mass (m/z,  $\pm 10$  ppm), retention time ( $\pm 30$  s), and MS/MS spectra for a level 1 identification as shown in [Table 2](#).<sup>28</sup> The SMI and mixed standards total ion chromatogram (TIC) are shown in [Figure 2A](#). Furthermore, the extracted ion chromatogram (EIC) of four components are presented in [Supplementary Figure 1](#). Finally, measured MS/MS spectral fragmentation profiles of SMI and standards were matched according to their accurate masses ([Figure 2B](#)).

**Table 3** Hub Genes and Topological Property

Gene Symbol	Protein Name	Average Shortest Path	Betweenness Centrality	Degree
IL6	Interleukin-6	1.3947	0.2066	23
STAT3	Signal transducer and activator of transcription 3	1.7747	0.1601	21
VEGFA	Vascular endothelial growth factor A	1.4737	0.2799	21
TNF	Tumor necrosis factor	1.6053	0.0588	17
MMP9	Matrix metalloproteinase-9	1.6316	0.0825	16
PTGS2	Prostaglandin G/H synthase 2	1.7105	0.0651	13
MMP2	Matrix metalloproteinase-2	1.7105	0.0176	13
ICAM1	Intercellular adhesion molecule 1	1.7105	0.022	12
MMP3	Matrix metalloproteinase-9	1.8421	0.0371	10
JAK2	Tyrosine-protein kinase JAK2	1.9474	0.0599	9
PTPRC	Receptor-type tyrosine-protein phosphatase C	1.9211	0.037	9
MMP1	Matrix metalloproteinase-1	1.8421	0.0058	9
ERBB2	Receptor tyrosine-protein kinase erbB-2	1.8421	0.0074	8
SERPINE1	Plasminogen activator inhibitor 1	1.8684	0.0136	8
HMOX1	Heme oxygenase 1	1.8947	0.0022	7



Using the predefined screening conditions, we obtained 770 candidate compound-related targets and 610 AP-related targets (Supplementary Table 3). PPI analysis yielded 59 potential therapeutic targets of SMI for treating AP (Figure 3A). The STRING database revealed the intersections among these potential therapeutic targets with a minimum required interaction score of 0.7 (high confidence). The PPI network comprised 49 nodes and 148 edges with an average node degree score of 6.04 (Figure 3B).

## Analysis of Related Pathways of Potential Targets

To gain more crucial targets, we calculated the betweenness centrality, shortest path, and degree of centrality of the target proteins using topological analysis. Targets with degree scores greater than the average value (6.04) were considered hub targets. Fifteen hub targets were screened for further exploration as the main targets of SMI in treating AP (Table 3,

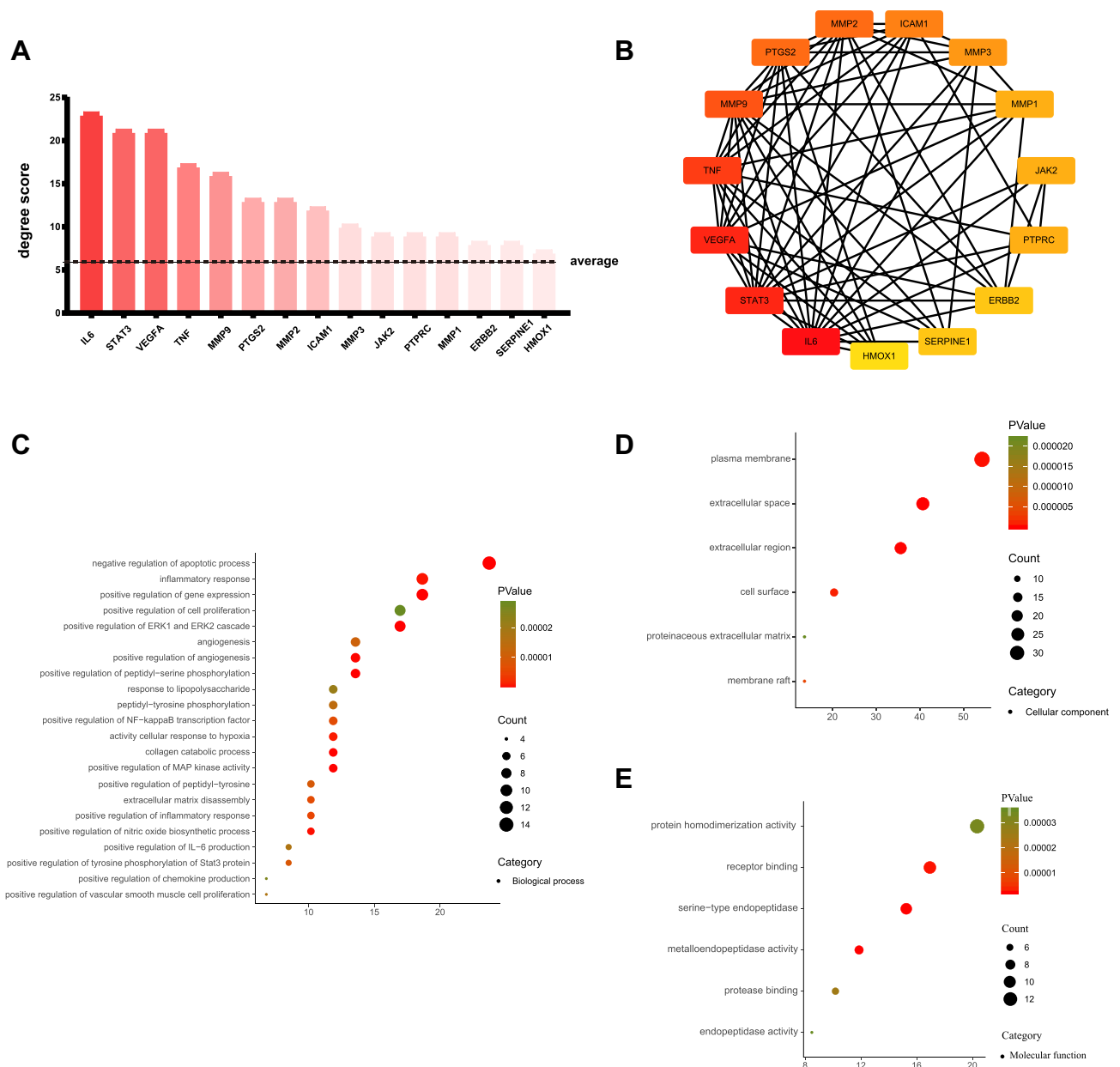


**Figure 4** GO enrichment analysis. (A) Histogram of hub gene degree scores. (B) Visual analysis of the hub genes in CytoHubba. (C–E) GO enrichment analysis of the hub genes from three aspects: biological process (BP), cellular component (CC) and molecular function (MF).  
**Abbreviation:** GO, Gene Ontology.

Figure 4A). Figure 4B provides a visual analysis of the 15 hub genes via CytoHubba, which highlights IL6 (degrees = 23) and STAT3 (degrees = 21) as the two main targets of SMI for the anti-inflammatory effects of AP. GO enrichment analysis revealed that the biological processes of the genes were highly enriched for apoptotic and inflammatory-related functions (Figure 4C). Figure 4D and E show the cellular components and molecular functions of the genes.

## Construction of IL6/STAT3-Related Subnetwork and Analysis of Compound Targets

A main compounds-targets-pathways network was constructed based on the four active components identified via UHPLC/MS, 15 hub targets selected from the PPI network, and eight pathways determined by KEGG analysis (Figure 5A).

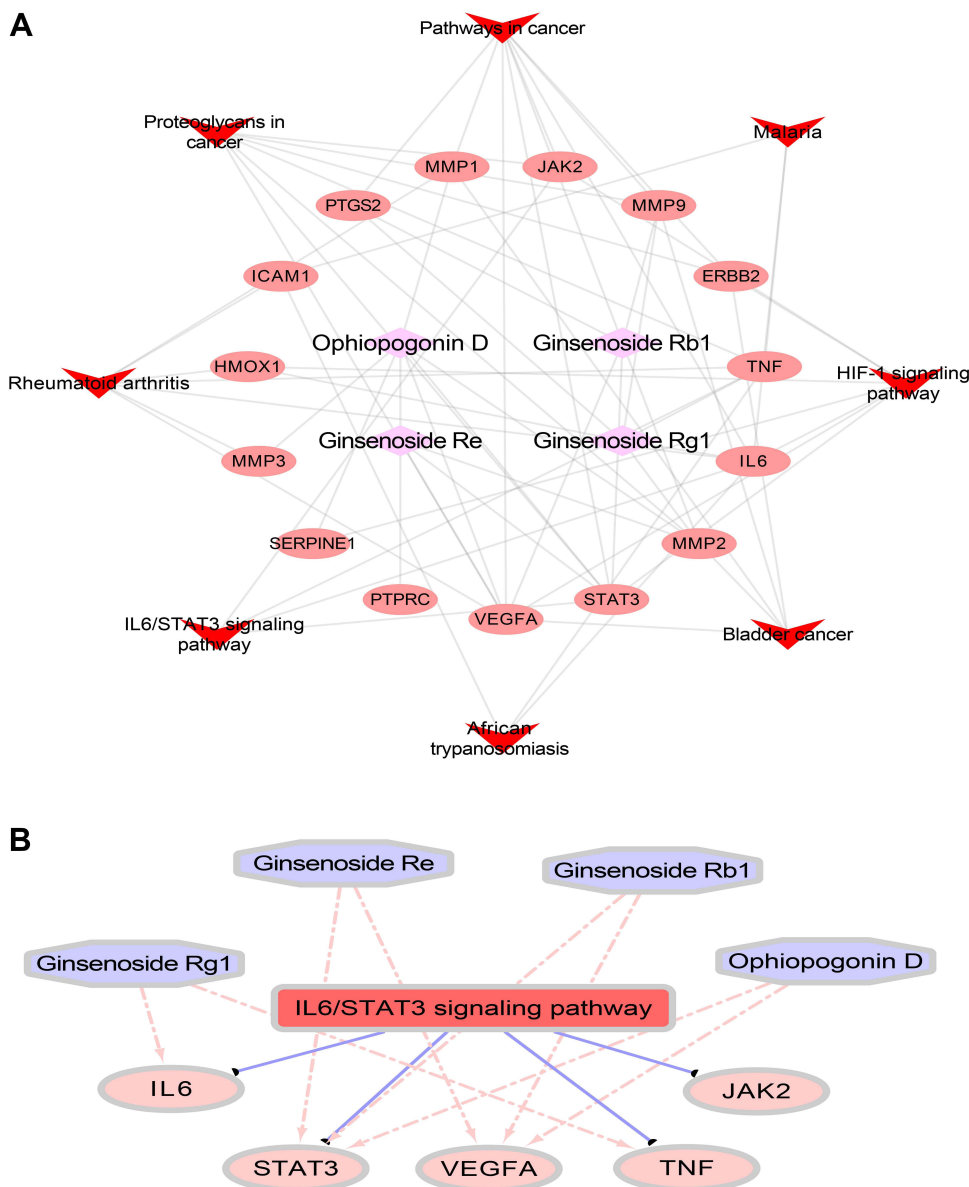


**Figure 5** Pharmacological network analysis. (A) The main compounds-targets-pathways network. (Diamonds represent the four active compounds; pink circles represent targets; red arrows represent KEGG pathways; edges indicate interactions between compounds and targets.). (B) Subnetwork of the four active compounds predicted to be targets of IL6, STAT3, TNF, and JAK2 related to the IL6/STAT3 pathway.

**Abbreviation:** KEGG, Kyoto Encyclopedia of Genes and Genomes.

To further evaluate the association between the main targets and the signaling pathways, we focused on the IL6/STAT3 inflammatory pathway to construct a subnetwork involving IL6, STAT3, Janus kinase (JAK) 2 and tumor necrosis factor (TNF) (Figure 5B). In the IL6/STAT3-related subnetwork, four active components of SMI (ginsenoside Rb1, ginsenoside Rg1, ginsenoside Re and ophiopogonin D) were predicted to have direct interactive functions with the top targets (IL6, STAT3, TNF, and JAK2). Ginsenoside Rg1 was predicted to regulate IL6 and TNF. Ginsenoside Re, ginsenoside Rb1, and ophiopogonin D were predicted to regulate STAT3 and VEGFA.

## Molecular Docking

Because IL6, STAT6, VEGFA, and TNF had the highest degrees in the topological analysis, we selected these genes and their corresponding components to evaluate their interactive activity by molecular docking. Table 4 shows the docking scores. Larger absolute docking affinity values indicated greater binding capability between the active sites of the targets and compounds. Figure 6 shows the molecular docking of IL6 and STAT3 with the four active components.

## SMI Attenuated NaT-Induced Cellular Injury

Next, we validated the anti-inflammatory effects of SMI on NaT-stimulated 266–6 cells. Here, 5 mM NaT decreased 266–6 cell viability by 60%, and SMI (1, 5, 10, and 20  $\mu\text{L}/\text{mL}$ ) helped regain viability of the NaT-stimulated 266–6 cells ( $p < 0.05$ ; Figure 7A). From the four doses, 5  $\mu\text{L}/\text{mL}$  SMI increased cell viability to ~80%. The four active components exerted different effects on the viability of the NaT-stimulated 266–6 cells (Figure 7B). Ginsenoside Re (100, 200, and 400  $\mu\text{M}$ ) increased the cell viability dose-dependently, with a maximal effect at 400  $\mu\text{M}$ . Ginsenoside Rb1 at 2 and 5  $\mu\text{M}$  and ginsenoside Rg1 at 50  $\mu\text{M}$  exerted the same effect. Ophiopogonin D did not appear to affect 266–6 cell viability.

## Effect of SMI on IL6/STAT3 Signaling in Acinar Cells

We next performed Western blot assays to validate the effect of SMI on IL6/STAT3 pathway in acinar cells (Figure 7C). NaT stimulation at 1 mM markedly upregulated the p-STAT3 and IL6 expressions ( $p < 0.01$ ). Expectedly, SMI treatment at 10  $\mu\text{L}/\text{mL}$  significantly decreased the p-STAT3 and IL6 levels compared with those of the AP-induced group ( $p < 0.01$ ). Figure 7D shows the quantitative analysis and comparison of the relative protein levels.

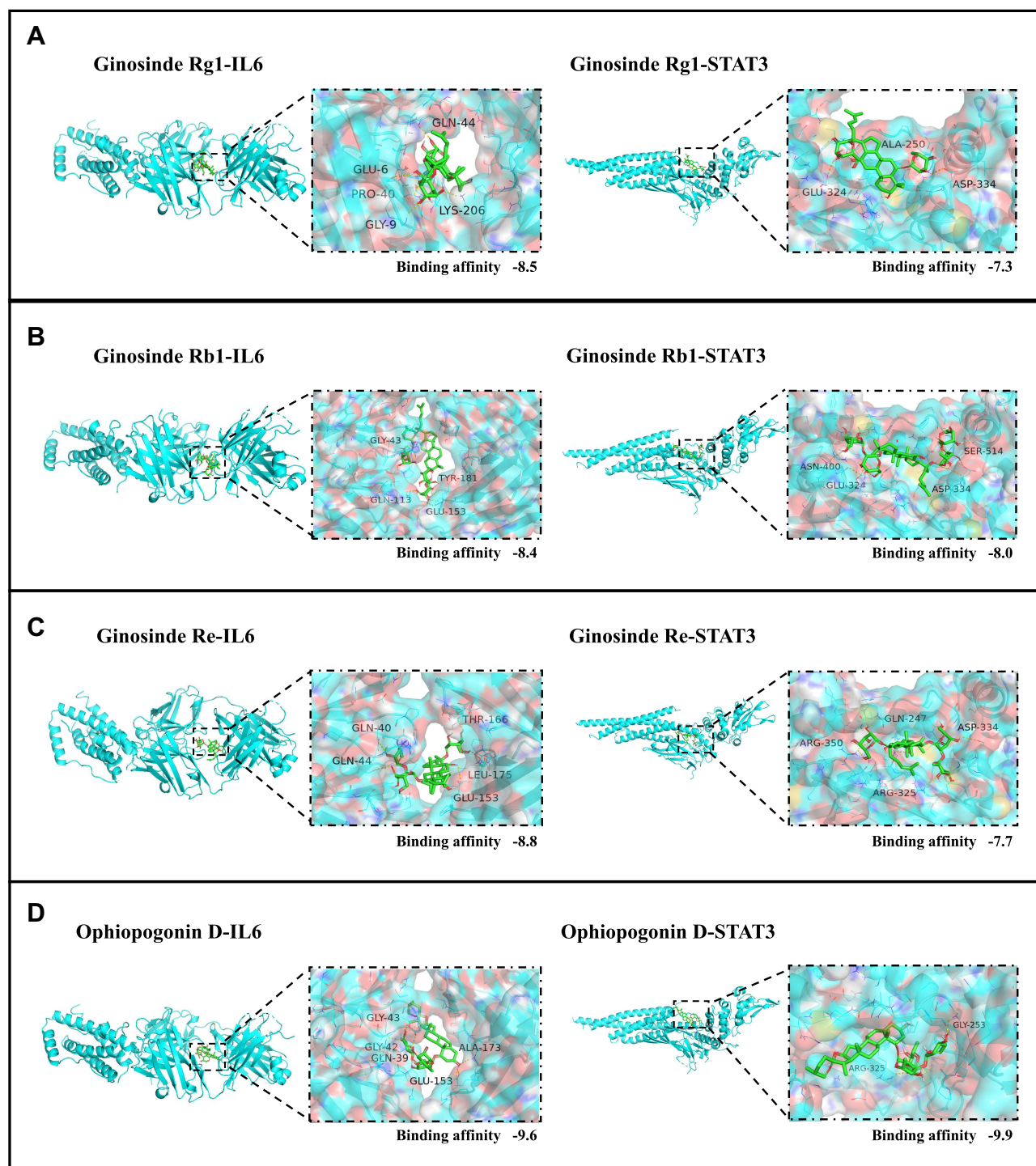
## Protective Effect of SMI on the Pathological Severity and IL6/STAT3 Activation in NaT-Induced AP Mice

Figure 8A shows the representative hematoxylin and eosin (H&E)-stained pancreatic images. 4%NaT successfully induced typical AP-associated histopathological changes manifesting as diffuse edema, neutrophil infiltration and acinar cell necrosis, as demonstrated by increased histopathological scores (Figure 8B). Pretreatment of SMI at 10 mL/kg significantly attenuated the histopathological scores of the AP-induced mice, indicating a protective effect of SMI for treating AP. 4%NaT successfully induced overexpression of p-STAT3 and IL6 in pancreatic tissues, and 10mL/kg SMI pretreatment reduced p-STAT3 and IL6 ( $p < 0.01$ ) (Figure 8C–D).

**Table 4** Binding Affinity Between Four Active Components from SMI and Potential Targets

Components	Binding Affinity (kcal/mol)			
	STAT3	VEGFA	IL6	TNF
Ginsenoside Rg1	-7.3	-7.7	-8.5	-6.1
Ginsenoside Re	-7.7	-7.8	-8.8	-6.7
Ginsenoside Rb1	-8	-8.1	-8.4	-7.3
Ophiopogonin D	-9.9	-9.1	-9.6	-8

**Abbreviations:** STAT3, signal transducer and activator of transcription 3; VEGFA, vascular endothelial growth factor a; IL6, Interleukin 6; TNF, tumor necrosis factor.



**Figure 6** Molecular docking models of the four active compounds binding to IL6 and STAT3 (A–D).

## Discussion

AP is a common digestive disease with no specific clinical interventions. TCM allows effectively and safely treating AP in clinical practice. Because “heat-evil” has been widely accepted in TCM as the main cause of AP, the principles of “clearing heat, removing toxins and purgation” should be followed and have been investigated. Heat-toxin progression may potentially harm Qi and Yin, and “clearing and purgation” treatment may cause or aggravate Qi and Yin deficiency. Based on this pathogenesis, we proposed that nourishing Qi and Yin should be an important adjunctive therapy in the

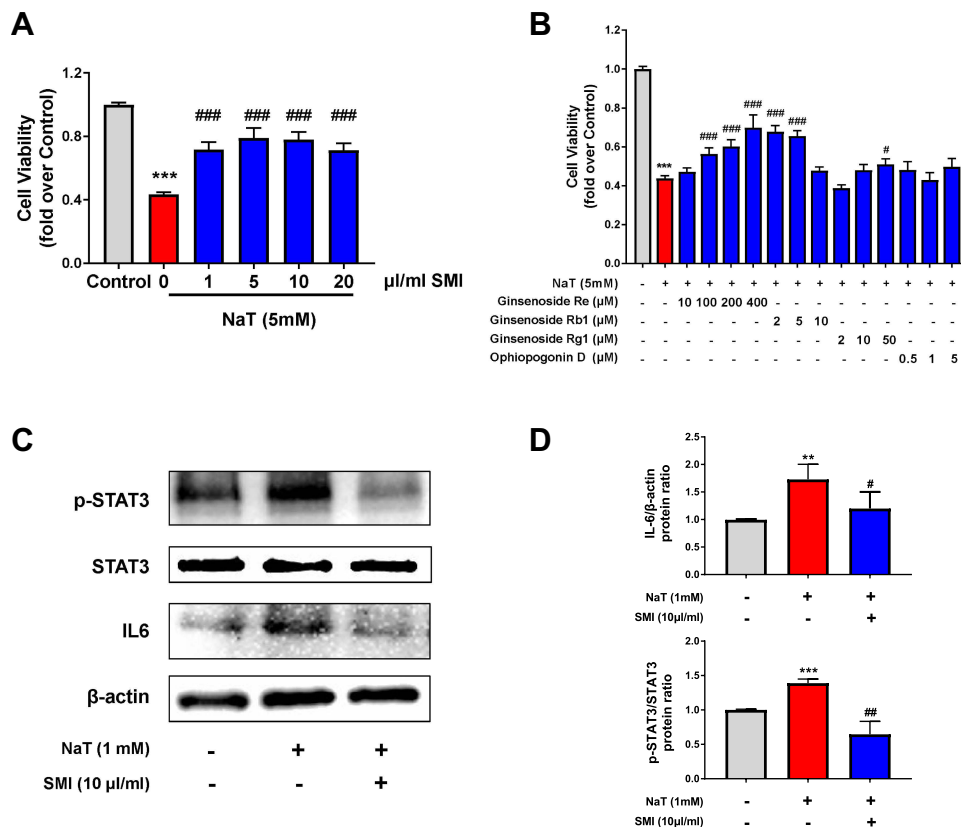


**Figure 7** Effects of SMI and compounds on cellular viability and IL6/STAT3. **(A)** Effects of SMI on viability of NaT-stimulated 266–6 cells. **(B)** Effects of the four active compounds on viability of NaT-stimulated 266–6 cells. **(C)** Representative Western blotting images for p-STAT3, STAT3, IL-6 and β-actin in 266–6 cells. **(D)** Relative expression levels of IL6 and p-STAT3 in each group. Data are expressed as the mean ± standard error from 4–5 independent experiments. \*\* $P < 0.01$ ; \*\*\* $P < 0.001$  vs control group, # $P < 0.05$ ; ## $P < 0.01$ ; ### $P < 0.001$  vs NaT group.

**Abbreviations:** SMI, Shenmai injection; NaT, sodium taurocholate.

early stages of AP. However, few studies have focused on this issue. SMI, extracted from *Panax ginseng* and *Ophiopogon japonicus*, is a frequently used extract for qi-yin deficiency.<sup>22,23</sup> In a previous study with a severe AP-induced rat model, SMI administration reduced the inflammatory indices, attenuated the histopathological severity of multiple organs, and activated HO-1 signaling.<sup>29</sup> In the present study, we for the first time performed an integrated strategy of active ingredient determination, network pharmacology, molecular docking and experimental validation to investigate the chemical basis and mechanisms of SMI.

In our study, component screening initially revealed 72 active compounds from *Panax ginseng* and 47 compounds from *Ophiopogon japonicus*, from which, we further determined the active components. Next, UHPLC-QTOF-MS analysis verified four active components of SMI (ginsenoside Rb1, ginsenoside Rg1, ginsenoside Re, and ophiopogonin D), which was consistent with previous reports.<sup>26,27</sup> Our experiment demonstrated that ginsenoside Rb1, ginsenoside Rg1 and ginsenoside Re effectively alleviated pancreatic acinar cellular injury. Ophiopogonin D appeared to exert no protective effect on reducing injury in cultured 266–6 cells. However, we did not detect the ratio and dosage of the four active ingredients in Shenmai injection, so the effective protective dose of active ingredients could not be achieved. Further studies are need for developing SMI-based pharmacological treatments for AP.

By using topological analysis and pharmacological subnetwork, we found four active components of SMI (ginsenoside Rb1, ginsenoside Rg1, ginsenoside Re and ophiopogonin D) would have direct interactive functions with IL6/STAT3. Furthermore, a detailed molecular docking approach revealed that these active components displayed good affinity for IL6 and STAT3. Our experimental studies demonstrated that SMI increased the viability of NaT-stimulated mouse pancreatic acinar cells and alleviated the pancreatic histopathological changes in the NaT-induced AP mice. Further, SMI decreased IL6 and STAT3 expressions both in vivo and in vitro. IL6,

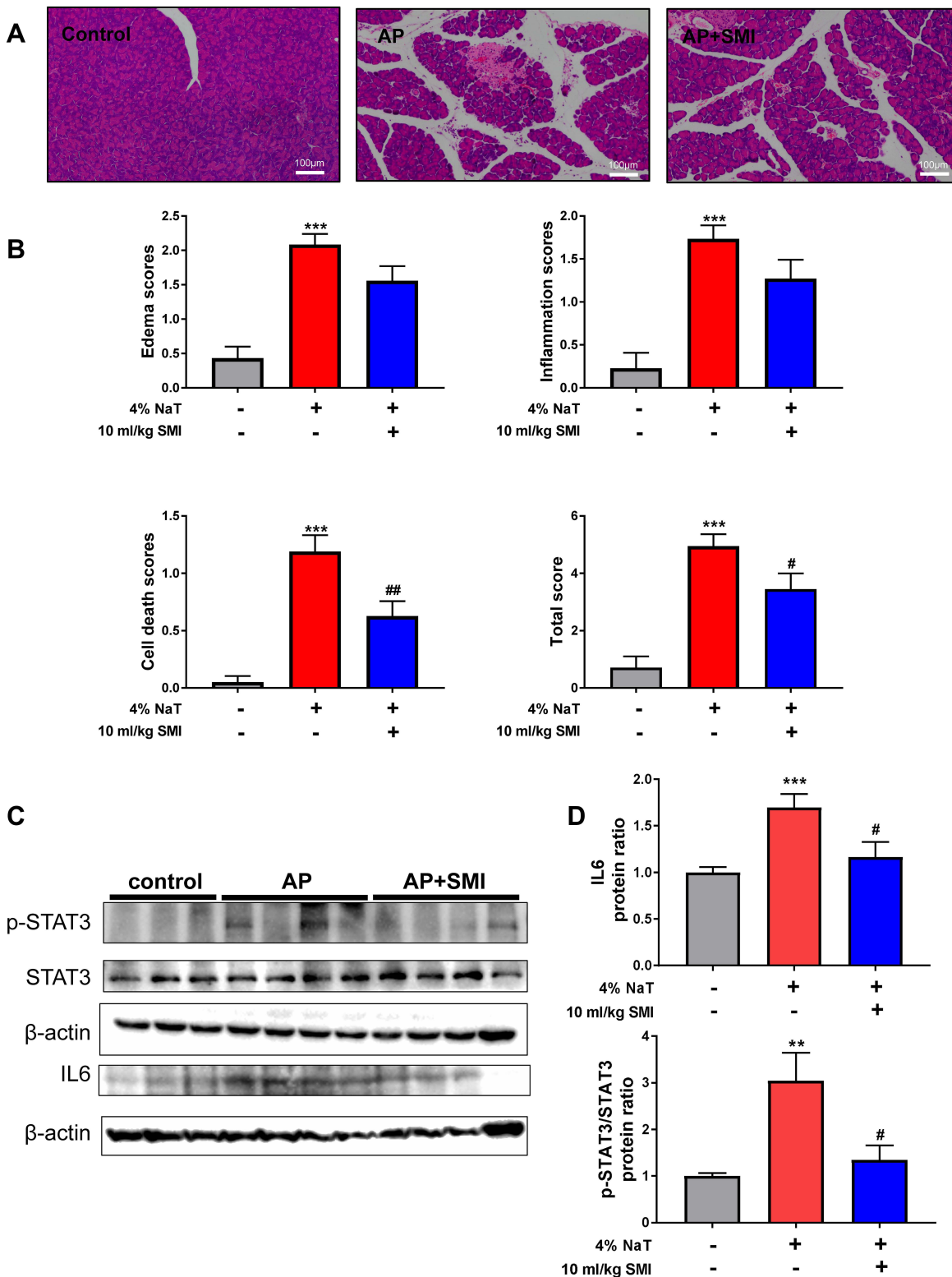


**Figure 8** Effects of SMI on the histopathological severity of NaT-induced AP in mice. **(A)** Representative H&E images of pancreatic sections (magnification 100 $\times$ ). **(B)** Pancreatic histopathology scores. **(C)** Representative Western blotting images of p-STAT3, STAT3 IL-6 and  $\beta$ -actin of pancreatic tissue. **(D)** Relative expression levels of corresponding proteins. Data are expressed as means  $\pm$  standard error from two independent experiments ( $n = 3-4$  per group). \*\* $P < 0.01$ ; \*\*\* $P < 0.001$  vs control group, # $P < 0.05$ ; ## $P < 0.01$  vs NaT group.

**Abbreviations:** SMI, Shenmai injection; NaT, sodium taurocholate; H&E, hematoxylin and eosin.

a proinflammatory cytokine, significantly increased and positively correlated with AP severity.<sup>30–32</sup> Circulating IL6 either binds to IL6R $\alpha$  and gp130 on target cells or binds to a soluble form of IL6R $\alpha$  (sIL6R) to form a complex that interacts with membrane-bound gp130, thus activating downstream JAKs and STAT3 by phosphorylating tyrosine 705.<sup>33</sup> Then STAT3 dimerizes and translocates to the nucleus to regulate its target genes. This positive feed-back loop amplifies the progression of the systemic inflammatory cascade during AP.<sup>34</sup> Neutralizing antibody against IL6 effectively inhibited STAT3 activation in the pancreas and reduced disease severity by promoting pancreatic acinar cell apoptosis.<sup>35</sup> Studies have shown that SMI has immunomodulatory effects against inflammatory injuries by suppressing mediators.<sup>25,36</sup> Ginsenosides are a class of steroid glycosides and triterpene saponins, which include over 40 members. Among them, ginsenoside Rb1, ginsenoside Rg1, and ginsenoside Re have been reported to ameliorate inflammatory injury by regulating the NF- $\kappa$ B signaling pathway and inflammatory mediators, including TNF- $\alpha$  and IL6.<sup>37–40</sup> We found tentative evidence for the protective effects of SMI by partially suppressing IL6/STAT3 activation. However, it remains unknown whether SMI regulates STAT3 nuclear translocation and its downstream targets. This research warrants further in-depth investigation to establish a potential pathway for developing novel drugs.

This study had several limitations. First, because we focused on the reported active components of SMI, the therapeutic effects of the other components of SMI may have been underestimated. Second, because medicinal material quality is the most important consideration for the product's effects, a single batch of the drug is insufficient. Although we developed a material quality control strategy, further studies are needed to validate the therapeutic effects of SMI and its components using different batches. Third, until recently, no consensus was available regarding the TCM syndrome that should be used in AP experimental models.

## Conclusion

In this study, we explored for the first time the bioactive components of the representative formula for “nourishing Qi and Yin” as well as SMI and its anti-inflammatory effects in the early stages of AP by using network pharmacology analysis, molecular docking and animal validation. Our results demonstrated that SMI alleviated the severity of experimentally induced AP partly by suppressing IL6/STAT3 activation, thus providing a basis for using SMI in clinical practice and further studying AP.

## Funding

This study was supported by the National Natural Science Foundation of China (No. 82104715, CH; No. 82074230, LD); Sichuan Province Science and Technology Support Program (No. 2020YJ0235, CH).

## Disclosure

The authors declare that there are no conflicts of interest.

## References

1. Peery AF, Crockett SD, Barritt AS, et al. Burden of gastrointestinal, liver, and pancreatic diseases in the United States. *Gastroenterology*. 2015;149(7):1731–1741 e1733. doi:10.1053/j.gastro.2018.08.063
2. Iannuzzi JP, King JA, Leong JH, et al. Global incidence of acute pancreatitis is increasing over time: a systematic review and meta-analysis. *Gastroenterology*. 2022;162(1):122–134. doi:10.1053/j.gastro.2021.09.043
3. Sarri G, Guo Y, Iheanacho I, Puelles J. Moderately severe and severe acute pancreatitis: a systematic review of the outcomes in the USA and European Union-5. *BMJ Open Gastroenterol*. 2019;6(1):e000248. doi:10.1136/bmjgast-2018-000248
4. Schepers N, Bakker O, Besselink M, et al. Impact of characteristics of organ failure and infected necrosis on mortality in necrotising pancreatitis. *Gut*. 2019;68(6):1044–1051. doi:10.1136/gutjnl-2017-314657
5. van Santvoort H, Bakker O, Bollen T, et al. A conservative and minimally invasive approach to necrotizing pancreatitis improves outcome. *Gastroenterology*. 2011;141(4):1254–1263. doi:10.1053/j.gastro.2011.06.073
6. Moggia E, Koti R, Belgaumkar A, et al. Pharmacological interventions for acute pancreatitis. *Cochrane Database Syst Rev*. 2017;4:CD011384. doi:10.1002/14651858
7. Crockett S, Wani S, Gardner T, Falck-Ytter Y, Barkun AN. American Gastroenterological Association Institute guideline on initial management of acute pancreatitis. *Gastroenterology*. 2018;154(4):1096–1101. doi:10.1053/j.gastro.2018.01.032
8. Vege S, DiMaggio M, Forsmark C, Martel M, Barkun AJG. Initial medical treatment of acute pancreatitis: American Gastroenterological Association Institute technical review. *Gastroenterology*. 2018;154(4):1103–1139. doi:10.1053/j.gastro.2018.01.031

9. Lu X, Xiao W, Kang X, Yu J, Fan Z. The effect of Chinese herbal medicine on non-biliogenic severe acute pancreatitis: a systematic review and meta-analysis. *J Ethnopharmacol.* 2014;155(1):21–29. doi:10.1016/j.jep.2014.05.040
10. Li J, Zhang S, Zhou R, Zhang J, ZJWjog L. Perspectives of traditional Chinese medicine in pancreas protection for acute pancreatitis. *World J Gastroenterol.* 2017;23(20):3615–3623. doi:10.3748/wjg.v23.i20.3615
11. Wen Y, Han C, Liu T, et al. Chaiqin chengqi decoction alleviates severity of acute pancreatitis via inhibition of TLR4 and NLRP3 inflammasome: identification of bioactive ingredients via pharmacological sub-network analysis and experimental validation. *Phytomedicine.* 2020;79:153328. doi:10.1016/j.phymed.2020.153328
12. Xia Q, Huang W, Jin T, Zhang X Chinese Association of Integrative Medicine, integrated traditional Chinese and Western medicine practice guidelines for diagnosis and treatment of acute pancreatitis; 2021. Available from: [http://www.caim.org.cn/info\\_content.jsp?id=8342](http://www.caim.org.cn/info_content.jsp?id=8342). Accessed July 22, 2022.
13. Chen W, Yang X, Huang L, et al. Qing-Yi decoction in participants with severe acute pancreatitis: a randomized controlled trial. *Chin Med.* 2015;10:11. doi:10.1186/s13020-015-0039-8
14. Liu XB, Jiang JM, Huang ZW, et al. 中西医结合治疗重症急性胰腺炎的临床研究 (附1376例报告). *Sichuan Da Xue Xue Bao Yi Xue Ban.* 2004;35(2):204–208. Chinese.
15. Lu M, Zhang Q, Chen K, Xu W, Xiang X, Xia S. The regulatory effect of oxymatrine on the TLR4/MyD88/NF- $\kappa$ B signaling pathway in lipopolysaccharide-induced MS1 cells. *Phytomedicine.* 2017;36:153–159. doi:10.1016/j.phymed.2017.10.001
16. Wei TF, Zhao L, Huang P, et al. Qing-Yi decoction in the treatment of acute pancreatitis: an integrated approach based on chemical profile, network pharmacology, molecular docking and experimental evaluation. *Front Pharmacol.* 2021;12:590994. doi:10.3389/fphar.2021.590994
17. Wu W, Luo R, Lin Z, Xia Q, Xue P. Key molecular mechanisms of chaiqinchengqi decoction in alleviating the pulmonary albumin leakage caused by endotoxemia in severe acute pancreatitis rats. *Evid Based Complement Alternat Med.* 2016;2016:3265368. doi:10.1155/2016/3265368
18. Xiang H, Zhang Q, Qi B, et al. Chinese herbal medicines attenuate acute pancreatitis: pharmacological activities and mechanisms. *Front Pharmacol.* 2017;8:216. doi:10.3389/fphar.2017.00216
19. Zhang CL, Lin ZQ, Luo RJ, et al. Chai-Qin-Cheng-Qi decoction and carbachol improve intestinal motility by regulating protein Kinase C-Mediated Ca(2+) release in colonic smooth muscle cells in rats with acute necrotising pancreatitis. *Evid Based Complement Alternat Med.* 2017;2017:5864945. doi:10.1155/2017/5864945
20. Zhang MJ, Zhang GL, Yuan WB, Ni J, Huang LF. Treatment of abdominal compartment syndrome in severe acute pancreatitis patients with traditional Chinese medicine. *World J Gastroenterol.* 2008;14(22):3574–3578. doi:10.3748/wjg.14.3574
21. Lu LY, Zheng GQ, Wang Y. An overview of systematic reviews of shenmai injection for healthcare. *Evid Based Complement Alternat Med.* 2014;2014:840650. doi:10.1155/2014/840650
22. Huang X, Duan X, Wang K, Wu J, Zhang X. Shengmai injection as an adjunctive therapy for the treatment of chronic obstructive pulmonary disease: a systematic review and meta-analysis. *Complement Ther Med.* 2019;43:140–147. doi:10.1016/j.ctim.2019.01.020
23. Wang X, Wu M, Lai X, et al. Network pharmacology to uncover the biological basis of spleen qi deficiency syndrome and herbal treatment. *Oxid Med Cell Longev.* 2020;2020:2974268. doi:10.1155/2020/2974268
24. Wei PF. Diagnosis and treatment protocol for novel coronavirus pneumonia (trial version 7). *Chin Med J.* 2020;133(9):1087–1095.
25. Zhang F, Liu Y, Dong X, et al. Shenmai injection upregulates heme oxygenase-1 to confer protection against severe acute pancreatitis. *J Surg Res.* 2020;256:295–302. doi:10.1016/j.jss.2020.06.035
26. Xia C, Wang G, Sun J, et al. Simultaneous determination of ginsenoside Rg1, Re, Rd, Rb1 and ophiopogonin D in rat plasma by liquid chromatography/electrospray ionization mass spectrometric method and its application to pharmacokinetic study of ‘SHENMAI’ injection. *J Chromatogr B Analyt Technol Biomed Life Sci.* 2008;862:72–78. doi:10.1016/j.jchromb.2007.11.020
27. Yu J, Li Y, Liu X, et al. Mitochondrial dynamics modulation as a critical contribution for Shenmai injection in attenuating hypoxia/reoxygenation injury. *J Ethnopharmacol.* 2019;237:9–19. doi:10.1016/j.jep.2019.03.033
28. Viant MR, Kurland IJ, Jones MR, Dunn WB. How close are we to complete annotation of metabolomes? *Curr Opin Chem Biol.* 2017;36:64–69. doi:10.1016/j.cbpa.2017.01.001
29. Li L, Li J, Wang Q, et al. Shenmai injection protects against doxorubicin-induced cardiotoxicity via maintaining mitochondrial homeostasis. *Front Pharmacol.* 2020;11:815. doi:10.3389/fphar.2020.00815
30. Jiang CF, Shiao YC, Ng KW, Tan SW. Serum interleukin-6, tumor necrosis factor alpha and C-reactive protein in early prediction of severity of acute pancreatitis. *J Chin Med Assoc.* 2004;67(9):442–446.
31. Khanna AK, Meher S, Prakash S, et al. Comparison of Ranson, Glasgow, MOSS, SIRS, BISAP, APACHE-II, CTSI scores, IL-6, CRP, and procalcitonin in predicting severity, organ failure, pancreatic necrosis, and mortality in acute pancreatitis. *HPB Surg.* 2013;2013:367581. doi:10.1155/2013/367581
32. Soyalp M, Yalcin M, Oter V, Ozgonul A. Investigation of procalcitonin, IL-6, oxidative stress index (OSI) plasma and tissue levels in experimental mild and severe pancreatitis in rats. *Bratisl Lek Listy.* 2017;118(3):137–141. doi:10.4149/BLL\_2017\_027
33. Baran P, Hansen S, Waetzig GH, et al. The balance of interleukin (IL)-6, IL-6-soluble IL-6 receptor (sIL-6R), and IL-6-sIL-6R-sgp130 complexes allows simultaneous classic and trans-signaling. *J Biol Chem.* 2018;293(18):6762–6775. doi:10.1074/jbc.RA117.001163
34. Zhang H, Neuhöfer P, Song L, et al. IL-6 trans-signaling promotes pancreatitis-associated lung injury and lethality. *J Clin Invest.* 2013;123(3):1019–1031. doi:10.1172/JCI64931
35. Chao K, Chao K, Chuang C, Liu S. Blockade of interleukin 6 accelerates acinar cell apoptosis and attenuates experimental acute pancreatitis in vivo. *Br J Surg.* 2006;93(3):332–338. doi:10.1002/bjs.5251
36. Zhang S, You ZQ, Yang L, et al. Protective effect of Shenmai injection on doxorubicin-induced cardiotoxicity via regulation of inflammatory mediators. *BMC Complement Altern Med.* 2019;19(1):317. doi:10.1186/s12906-019-2686-2
37. Jiang Y, Zhou Z, Meng QT, et al. Ginsenoside Rb1 treatment attenuates pulmonary inflammatory cytokine release and tissue injury following intestinal ischemia reperfusion injury in mice. *Oxid Med Cell Longev.* 2015;2015:843721. doi:10.1155/2015/843721
38. Lim KH, Lim DJ, Kim JH. Ginsenoside-Re ameliorates ischemia and reperfusion injury in the heart: a hemodynamics approach. *J Ginseng Res.* 2013;37(3):283–292. doi:10.5142/jgr.2013.37.283
39. Tao T, Chen F, Bo L, et al. Ginsenoside Rg1 protects mouse liver against ischemia-reperfusion injury through anti-inflammatory and anti-apoptosis properties. *J Surg Res.* 2014;191(1):231–238. doi:10.1016/j.jss.2014.03.067
40. Zhao J, He B, Zhang S, Huang W, Li X. Ginsenoside Rg1 alleviates acute liver injury through the induction of autophagy and suppressing NF- $\kappa$ B/NLRP3 inflammasome signaling pathway. *Int J Med Sci.* 2021;18(6):1382–1389. doi:10.7150/ijms.50919



Drug Design, Development and Therapy

Dovepress

### Publish your work in this journal

Drug Design, Development and Therapy is an international, peer-reviewed open-access journal that spans the spectrum of drug design and development through to clinical applications. Clinical outcomes, patient safety, and programs for the development and effective, safe, and sustained use of medicines are a feature of the journal, which has also been accepted for indexing on PubMed Central. The manuscript management system is completely online and includes a very quick and fair peer-review system, which is all easy to use. Visit <http://www.dovepress.com/testimonials.php> to read real quotes from published authors.

Submit your manuscript here: <https://www.dovepress.com/drug-design-development-and-therapy-journal>